PROCEEDINGS OF SCIENCE

Accessing the forward region of the energy spectrum of leading neutral pions in ultra-high energy proton-Air interactions

Miguel Alexandre Martins,[a,b,*] **Lorenzo Cazon,**[a] **Ruben Conceição**[b] **and Felix Riehn**[a]

[a] *Instituto Galego de Física de Altas Enerxías,*
Rúa de Xoaquín Díaz de Rábago, s/n, Campus Vida, Universidade de Santiago de Compostela 15705 Santiago de Compostela, Galicia, Spain

[b] *Laboratório de Instrumentação e Física Experimental de Partículas,*
Av. Prof. Gama Pinto, n.2, 1649-003 Lisboa, Portugal

E-mail: miguelalexandre.jesusdasilva@usc.es

Ultra-high energy cosmic rays interact with nuclei of the Earth's atmosphere at $\sim 10 \times \sqrt{s}$ of proton-proton collisions at the LHC and in extremely high rapidity regions, providing a unique opportunity to probe hadronic interactions in poorly explored regions of the kinematic phase space of p-air interactions.

In this contribution, we show that fluctuations in the muon content of Extensive Air Showers correlate with fluctuations of the fraction of the primary energy that goes into hadronic channel of the primary p-air interaction. Furthermore, we show that measurements of the slope of the low tail of the muon number distribution in EAS constrain the forward inclusive cross-section for the production of neutral pions in-pair interactions at $\sim$ 450 TeV.

Moreover, we explore the joint $X_{\rm max} - N_\mu$ distribution, demonstrating that the slope of the tail of the muon number distribution is sensitivity to $X_{\rm max}$, in such a way that hadronic models converge for shallower $X_{\rm max}$ and diverge for deeper showers. In particular, we hint at the connection between these regimes and the presence of diffraction in p-air interactions.

38th International Cosmic Ray Conference (ICRC2023)
26 July - 3 August, 2023
Nagoya, Japan

*Speaker

PoS(ICRC2023)448

1. Introduction

The highest energy hadronic interactions in Extensive Air Showers (EAS) initiated by Ultra-high-energy Cosmic Rays (UHECR) with $E_0 > 1$ EeV, far exceed the energy and rapidity values reached in human-made colliders [1], providing an opportunity to constrain QCD interactions in poorly explored regions of the kinematic phase space of p-air collisions.

In UHECR experiments, the primary energy and arrival direction are reconstructed from shower observables, and its mass composition is inferred in a model-dependent way, using EAS simulations, based on different hadronic interaction models. These models, such as Epos-lhc [2], QGSJet II-04 [3] and Sibyll 2.3d [4], employ different physical mechanisms in extrapolating data obtained with colliders at lower energy and rapidity, and lead to large systematic uncertainties and inconsistencies in the interpretation of shower observables. In this context, a deficit in the average number of muons in EAS, $\langle N_\mu \rangle$, is found in simulations, the so-called Muon Puzzle [5] though fluctuations of N_μ as measured by the Pierre Auger Observatory (PAO) [6] agree with model predictions [7]. Thus, testing hadronic interaction models within and outside the kinematic phase space regions covered by forward colliders [8], is crucial to understand the origin of the muon puzzle and pinpoint where models start to diverge.

Information regarding the primary composition and hadronic interactions is encoded in the shower-to-shower distributions of the number of muons at the ground, N_μ, and the depth of the maximum of the electromagnetic cascade, $X_{\rm max}$. Muons arise from the hadronic decay, and travel from their production point to the ground carrying information about the underlying hadronic activity of the EAS, while $X_{\rm max}$ moments evolve with the primary composition. The combination of these observables improves sensitivity to the primary composition [9] and tests the consistency of hadronic interaction models. Moreover, the shapes of the distributions of N_μ and $X_{\rm max}$, constrain those of macroscopic kinematic variables of the highest energy p-air interactions [10].

In this contribution, we show that the slope of the low tail of the distribution of N_μ in proton-initiated EAS constrains the shape of the energy spectrum of hadrons in the first p-air interaction, and, more fundamentally, the forward inclusive cross section for the production of neutral pions. By selecting cuts in $X_{\rm max}$, we show that the slope of the low tail of the muon number distribution becomes model dependent for deeper showers and universal for shallower ones. We hint that this behavior is related to the interplay between deeply inelastic and elastic first interactions.

2. Probing the energy spectrum of hadrons in p-air interactions at $\sqrt{s} \sim 450$ TeV

In the framework of the Heitler-Mathews (H-M) model [11] the average muon content in proton-initiated EAS is related to the primary energy E_0, via

$$\langle N_\mu \rangle = C E_0^\beta, \text{ with } \beta = \frac{\ln m}{\ln m_{\rm total}}, \tag{1}$$

where m designates the multiplicity of hadronically interacting particles and $m_{\rm total}$ the total multiplicity. In the original model, these are assumed to be constant for each interaction. In models, $\beta \sim 0.93$, and $C \sim \left(\xi_c^\pi\right)^{-\beta}$ where $\xi_c^\pi \sim 100$ GeV is the critical energy of charged pions. Note that N_μ is meant to represent the total number of muons produced, and not at the ground, even though the latter can be used if propagation effects are accounted for by C.

In [12], the H-M model is extended by including stochastic fluctuations of multiplicity and sharing of energy in each hadron-air interaction, and assessing their impact on fluctuations of N_μ. By defining a modified fraction of energy in the hadronic channel for the first shower generation[1],

$$\alpha_1 = \sum_{i=1}^{m} \left(\frac{E_{\rm had}}{E_0} \right)^{\beta}, \tag{2}$$

and the same for all generations, we can express N_μ as $N_\mu(E_0) = \langle N_\mu(E_0) \rangle \prod_{g=1}^{g_c} \alpha_g = \alpha_1 \omega$, where ω encompasses all generations but the first and g_c is the average critical generation. It was then shown that

$$\frac{\sigma(N_\mu)}{N_\mu} \simeq \frac{\sigma(\alpha_1)}{\alpha_1}, \tag{3}$$

where $\sigma(X)$ is the width of the distribution of the random variable X. Hence, the distribution of N_μ in EAS directly probes the energy spectrum of hadrons of the most energetic p-air interaction. In fact, in [13] it is additionally demonstrated that the symmetrical shape of $f_{\alpha_1, N_\mu}(\alpha_1, N_\mu)$, allows the probing of the tail of $f_{\alpha_1}(\alpha_1)$ via the shape of $f_{\ln N_\mu}(\ln N_\mu)$

Here, the connection between α_1 and N_μ, is demonstrated with 10^6 CONEX [14] simulations of proton initiated EAS, with primary energy $E_0 = 10^{19}$ eV and zenith angle $\theta = 67°$, produced for the hadronic interaction models: EPOS-LHC, QGSJET II-04 and SIBYLL 2.3d. The number of muons with $E_\mu > 1$ GeV is measured from the muon longitudinal profile at 1 400 meters a.s.l, the average altitude of PAO [6]. The low tails of $f_{\alpha_1}(\alpha_1)$ and $f_{\ln N_\mu}(\ln N_\mu)$ are fitted to exponential functions, $y = A\mathrm{e}^{\alpha_1/\Lambda_\alpha}$ and $y = B\mathrm{e}^{\ln N_\mu/\Lambda_\mu}$, respectively, where Λ_α and Λ_μ are the exponential slopes of the tails of the respective distributions. The upper limits of fit ranges correspond to the 20% and 10% percentiles of $f_{\alpha_1}(\alpha_1)$ and $f_{\ln N_\mu}(\ln N_\mu)$ respectively. The tails are fitted iteratively, starting at the bottom and raising the lower limit of the fit, bin by bin, until $\chi^2 < 2$. We verified that the fit converges each iteration and that the final fit range is representative of the extension of the tails of the distributions. As in [13], the connection between Λ_μ and Λ_α is demonstrated by modifying the distribution of α_1 below $\alpha_1 = 1$ by the transformation $f_{\alpha_1}(\alpha_1) \to \tilde{f}_{\alpha_1}(\alpha_1) = f_{\alpha_1}(\alpha_1)\mathrm{e}^{\delta\Lambda_\alpha(\alpha_1 - 1)}$ where $\delta\Lambda_\alpha$ is a small perturbation, under which $\Lambda_\alpha^{-1} \to \Lambda_\alpha^{-1} + \delta\Lambda_\alpha$, so that the frequency of events with $\alpha_1 < 1$ is exponentially suppressed. Thus, in each bin $\mathrm{d}\alpha_1$, k events can be sampled from the original $n \geq k$ set of events, and the corresponding values of N_μ stored. If $k > n$, then the same event is kept more than once. Repeating the process for all bins of α_1 yields a modified distribution of N_μ. The tails of the modified distributions are re-fitted and the new values of their slopes are extracted. We note that this is an ad-hoc procedure that does not try to replicate a physical change, and assumes that all correlations between α_1 and N_μ with other multi-particle production features are unchanged.

The left panel of Figure 1 shows the values of Λ_μ corresponding to Λ_α for each perturbation on the latter, while the right panel shows the nominal and modified distributions of α_1 and $\ln N_\mu$, for EPOS-LHC. Notably, Λ_μ responds linearly to changes in Λ_α, and in the same way for all hadronic interaction models, reflecting the similar relationship between tails of both distributions across models. In particular, the EPOS-LHC and SIBYLL 2.3d lines coincide. Furthermore, it is clear that

[1]The first generation comprises all secondaries of the primary interaction, $g = 2$ encompasses secondaries from interactions of $g = 1$, and so on, up to a critical generation g_c where the probability of decay surpasses that of interaction.

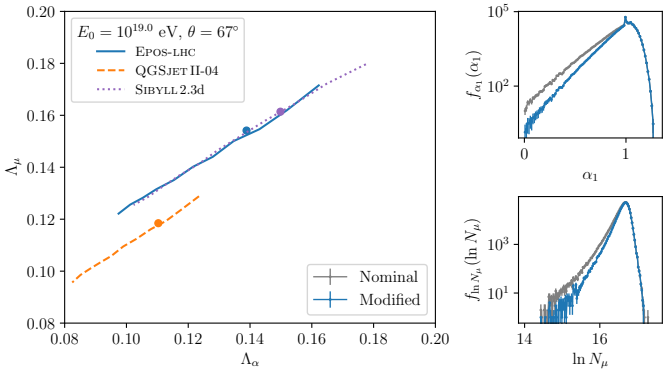

Figure 1: Left panel: Mapping between Λ_α and Λ_μ parametrized by an *ad-hoc* perturbation to Λ_α, for proton induced EAS simulated with CONEX with $E_0 = 10^{19}$ eV and $\theta = 67°$ for EPOS-LHC, QGSJET II-04 and SIBYLL 2.3d. Upper right panel: original and modified distribution of α_1 for EPOS-LHC. Lower right: original and modified distribution of $\ln N_\mu$ for EPOS-LHC, for a specific perturbation to $f_{\alpha_1}(\alpha_1)$.

measurements of Λ_μ can greatly constrain the possible values of Λ_α, within the uncertainty of the models. A measurement of this kind would thus probe the hardness of the energy spectrum of hadrons in p-air interactions in kinematic phase regions unexplored in human-made colliders. The feasibility of a measurement of Λ_μ for different primary composition scenarios, including detector resolutions for current UHE cosmic ray experiments is studied in [13].

3. Constraining the forward inclusive cross-section of π^0 in p-air interactions

If f_{had} is the fraction of energy carried by hadronically interacting particles of the primary interaction, one can take the approximations $\alpha_1 \simeq f_{\text{had}} \sim 1 - f_{\pi^0}$, with f_{π^0} the energy carried by neutral pions, in the lab. frame. Due to isopsin symmetry, the bulk of π^0 carries about $1/3$ of the total energy in the pionic sector. However, when fast neutral pions hadronize from valence quarks, the fraction of the primary energy carried by the leading π^0, x_{L}, obeys $x_{\text{L}}/f_{\pi^0} \sim 1$, and so

$$\alpha_1 \simeq 1 - x_{\text{L}} \implies \sigma(\alpha_1) \simeq \sigma(x_{\text{L}}) \implies \frac{\sigma(N_\mu)}{N_\mu} \simeq \frac{\sigma(x_{\text{L}})}{1 - x_{\text{L}}}. \tag{4}$$

For these events, the energy spectrum of leading neutral pions probes the forward energy spectrum of neutral pions. Furthermore, when fast neutral pions are produced, the energy available in the hadronic channel for the production of muons decreases, resulting muon poor events. In fact using the approximations $N_\mu \propto \alpha_1 \simeq 1 - x_{\text{L}}$, and denoting the proton-air inelastic cross section by $\sigma_{\text{p-air}}$, the inclusive cross-section for the production of neutral pions in p-air interactions by $\sigma_{\text{p-air}\to\pi^0}$ and the energy spectrum of leading neutral pions by $f_{x_{\text{L}}}(x_{\text{L}})$, leads to

$$f_{N_\mu}(N_\mu) \propto f_{\alpha_1}(\alpha_1) \simeq -f_{x_{\text{L}}}(x_{\text{L}}) \simeq -\frac{1}{\sigma_{\text{p-air}}} \frac{\mathrm{d}\,\sigma_{\text{p-air}\to\pi^0}}{\mathrm{d}x_{\text{L}}}. \tag{5}$$

Thus, the low tail of the distribution of N_μ should be related to the tail of the forward region of the energy spectrum of neutral pions. The correlation with the remaining energy spectrum of neutral pions worsens for low x_{L}, due to proton diffraction.

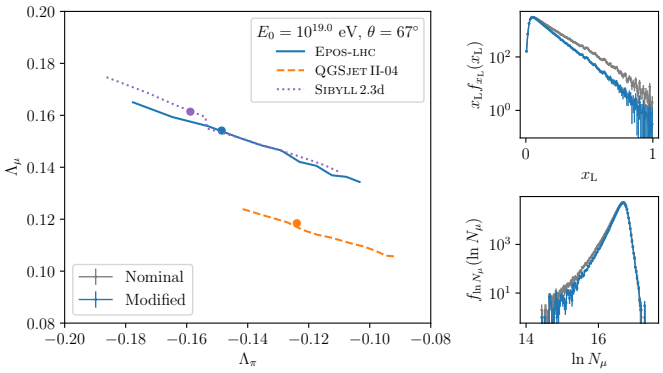

Figure 2: Left panel: Mapping between Λ_π and Λ_μ parametrized by an *ad-hoc* perturbation to Λ_π, for proton induced EAS simulated with Conex with $E_0 = 10^{19}$ eV and $\theta = 67°$ for Epos-lhc, QGSJet II-04 and Sibyll 2.3d. Upper right panel: original and modified energy spectra of leading neutral pions in the lab. frame for Epos-lhc. Lower right: original and modified distribution of $\ln N_\mu$ for Epos-lhc, for a specific perturbation to the forward region of the energy spectrum of neutral pions.

To test this reasoning, we build the distribution of $x_L f(x_L)$ over the ensemble of events, since its tail is rather exponential, and fit it to the function $y = Ce^{x_L/\Lambda_\pi}$, with the criteria discussed in Section 2. We then change the slope Λ_π, and repeat the sampling procedure described in the previous section, extracting, for each perturbation, the value of Λ_μ.

Figure 2 shows the response of Λ_μ to each perturbation on Λ_π. Though all models behave similarly, in the sense that a change $\delta\Lambda_\pi$ induces the same linear change in Λ_μ, the separation between models mirrors the poorer correlation between N_μ and x_L. Even so, the considered hadronic models span a small portion of the Λ_π-Λ_μ plane, meaning that a precise measurement Λ_μ could constrain the hardness of the energy spectrum of neutral pions of the first p-air interaction. This is the first time that features of the distribution of the number of muons, besides its moments, were used to probe hadronic interactions, possibly constraining the causes of the muon puzzle. We refer to [13] for details regarding the feasibility of the measurement of Λ_μ. Finally, an *a-priori* change on the spectrum of neutral pions is foreseen is a future publication.

4. Exploring kinematics of p-air UHE interactions in the $X_{\max}$-N_μ plane

The anti-correlation between $X_{\max}$-N_μ for a mixed composition can be partially explained by the Heilter-Mathews model. In this framework, $\langle X_{\max}\rangle_A$ and $\langle N_\mu\rangle_A$ for a primary with mass A can be related to those of a proton primary using the superposition principle,

$$\langle X_{\max}\rangle_A = \langle X_{\max}\rangle_p - \lambda_r \ln A\ , \quad \frac{\langle N_\mu\rangle_A}{\langle N_\mu\rangle_p} = A^{1-\beta} \implies \langle X_{\max}\rangle_A = -\frac{\lambda_r}{1-\beta}\ln\frac{\langle N_\mu\rangle_A}{\langle N_\mu\rangle_p} + \langle X_{\max}\rangle_p\ , \quad (6)$$

where λ_r is the radiation length. However, for a proton primary this anti-correlation is still present, as shown in middle panel of Figure 3 for Epos-lhc and in contour plots for $X_{\max}$-N_μ, on the right panel, for three hadronic interaction models, with the corresponding Pearson correlation coefficients.

Intuitively, the more energy that goes into the hadronic channel, the more muons are produced and less energy goes into neutral pions, triggering lower energy photon showers, lowering $X_{\max}$.

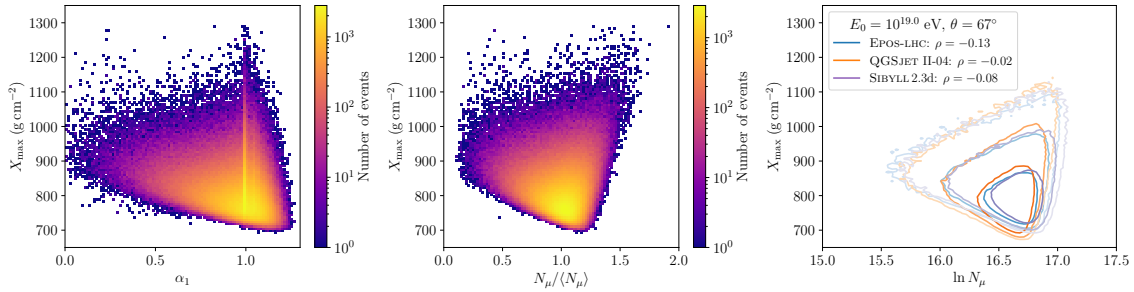

Figure 3: Left panel: joint $\alpha_1 - X_{\max}$ distribution for Epos-lhc. Middle panel: joint N_μ-$X_{\max}$ for Epos-lhc. Right panel: contours of the ln N_μ-$X_{\max}$ plane for the three hadronic interaction models Epos-lhc, QGSJet II-04 and Sibyll 2.3d. All distributions are built for an ensemble of 10^6 proton EAS simulated with Conex with $E_0 = 10^{19}$ eV and $\theta = 67°$.

Additionally, the enhancement of the multiplicity of hadronic interactions induces a faster shower development further, lowering $X_{\max}$. On the other hand, the enhanced decay of muons in older showers, leads to a decrease of N_μ, promoting a positive correlation with $X_{\max}$. This effect is clear when one considers the $X_{\max}$-α_1 plane, as shown in the left panel of Figure 3, which shows a stronger anti-correlation between $X_{\max}$ and α_1. In fact, the older the shower, the greater the fraction of decayed muons, transforming the inwards slanted right edge of the $X_{\max} - \alpha_1$ joint distribution into the outwards slanted right edge of the $X_{\max} - N_\mu$ joint distribution. Moreover, fluctuations of the depth of the first interaction, uncorrelated with the subsequent shower development, worsen the correlation between $X_{\max}$ and N_μ. Furthermore, in vertical showers the correlation between N_μ and $X_{\max}$ is affected by the truncation of the development of the electromagnetic and muon profiles. Importantly, the complexity of the connection between N_μ and $X_{\max}$ was explored in [10] to extract information about hadronic interactions. Finally, the left panel of Figure 3 shows that the joint $X_{\max} - N_\mu$ distribution is model dependent.

The shape of $f_{N_\mu, X_{\max}}(N_\mu, X_{\max})$ indicates that for each value of $X_{\max}$ there is a clear lower limit on N_μ. The same holds true for α_1. The exact origin of the this lower limit is not yet understood. However, since shallower showers are correlated with a higher multiplicity in the highest energy interactions, from $X_{\max} \sim -\ln m_{\text{total}}$, this limit might be related with kinematically forbidden regions of the α_1-m_{total} plane. This is under investigation.

To test the additionally constraints on first interaction properties impose by $X_{\max}$, we produce the distribution of N_μ and that of α_1, for cuts in $X_{\max}$, and fit the lower tail of the former to an exponential function, as discussed in Section 2. The evolution of Λ_μ with $X_{\max}$ is shown in the upper left panel Figure 4. The lower left panel displays, the average, 1% and 99% percentiles of $f_{\ln N_\mu}(\ln N_\mu)$ for cuts in $X_{\max}$, while the right panels show $f_{\alpha_1}(\alpha_1|X_{\max})$ and $f_{\ln N_\mu}(\ln N_\mu|X_{\max})$ for $X_{\max} \in \{[650, 750], [750, 800], [800, 850], [850, 900], [900, \infty]\}$ g cm^{-2}, such that darker shades of blue denote deeper showers, for Epos-lhc. The distributions marginalising $X_{\max}$ are depicted by a dashed grey line.

Concerning $f_{\alpha_1}(\alpha_1|X_{\max})$, it is clear that the the exponential tail is only present for deeper showers, and that its steepness decreases with $X_{\max}$, meaning that these contribute the most to the lower tail of α_1. Moreover, the peak at α_1 is not present in the shallowest bin of $X_{\max}$ and becomes

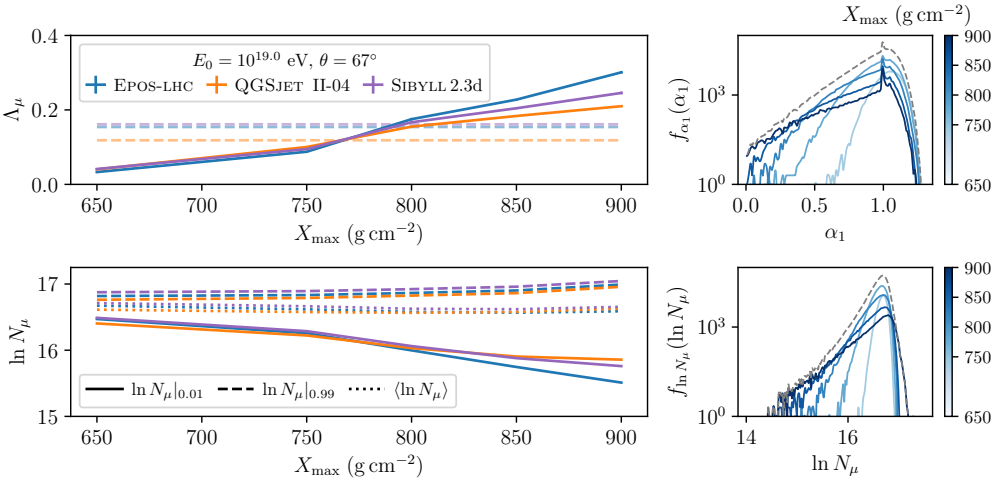

Figure 4: Upper left panel: evolution of Λ_μ for cuts in $X_{\max}$ for EPOS-LHC, QGSJET II-04 and SIBYLL 2.3d. Lower left panel: evolution of the average, 1% and 99% percentiles of the distribution of $\ln N_\mu$ for cuts in $X_{\max}$. Upper right panel: distribution of α_1 for cuts in $X_{\max}$ in shades of blue such that darker hues correspond to deeper $X_{\max}$, along with the total distribution represented as a dashed grey line, for EPOS-LHC. Lower right panel: distribution of $\ln N_\mu$ for cuts in $X_{\max}$ in shades of blue such that darker hues correspond to deeper $X_{\max}$, along with the total distribution represented as a dashed grey line, for EPOS-LHC. All distributions are built for an ensemble of 10^6 proton EAS simulated with CONEX with $E_0 = 10^{19}$ eV and $\theta = 67°$.

more pronounced for deeper showers, reflecting the fact that deeper showers are connected to highly elastic first interactions. Furthermore, there is a clear lower limit on α_1 for each bin in $X_{\max}$, that decreases for deeper showers.

On the other hand, the distribution $f_{\ln N_\mu}(\ln N_\mu | X_{\max})$, displays an exponential tail, irrespective of $X_{\max}$, that is flatter for deeper showers. The lower limit on N_μ for each cut in $X_{\max}$ decreases with $X_{\max}$, in connection with the minimum value of α_1. Most importantly, the slope of the low tail of $f_{\ln N_\mu}(\ln N_\mu | X_{\max})$ for shallower showers in model independent, while for deeper showers the models diverge. This appears to be related with the type of events of the first interaction being selected by $X_{\max}$: highly elastic p-air interactions probe phase-space regions of the interaction less constrained by accelerator data, leading to a more uncertain extrapolation carried out by the models. Conveniently, deeper showers correspond precisely with proton showers, allowing for a better measurement of Λ_μ in this regime, provided there are enough events. These claims must be thoroughly tested, despite being clear that $X_{\max}$ further constrains kinematic properties of the first interaction.

5. Conclusions and outlook

We showed that the hardness of the energy spectrum of hadronically interacting particles of p-air interactions at $E_0 = 10^{19}$ eV can be greatly constrained by measurements of the slope of the distribution of the number of muons in muon-poor proton showers, Λ_μ. Furthermore, we showed that the shape of the forward inclusive cross-section for the production of neutral pions in p-air interactions, is sensitive to Λ_μ, establishing the importance of a measurement of Λ_μ, both at the

highest energies and in the kinematic phase-space region probed by forward detectors, such as LHCf.

Furthermore, we have claimed that by selecting cuts in $X_{\rm max}$, we are separating different kinds of p-air first interactions with respect to their macroscopic production properties, and thus probing different regions of their kinematic phase space. In fact, we have showed that the deeper the shower, the greater the model separation regarding Λ_μ, motivating the importance of including $X_{\rm max}$ in constraining hadronic interactions at the highest energies.

6. Acknowledgements

The authors thank the fruitful discussions with Isabel Goos and Tanguy Pierog, pertaining to their preliminary work on the $X_{\rm max} - N_\mu$ correlation for proton-initiated EAS. MAM is also thankful for all the ideas that came up through discussions with Giuseppe Piparo and Alessio Tiberio.

This work has received financial support from Xunta de Galicia (CIGUS Network of Research Centers) and FCT - Fundação para a Ciência e a Tecnologia, I.P., under project CERN/FIS-PAR/0020/2021. MAM acknowledges that the project that gave rise to these results received the support of a fellowship from "la Caixa" Foundation (ID 100010434). The fellowship code is LCF/BQ/DI21/11860033. LC wants to thank financial support from Xunta de Galicia (Centro singular de investigacion de Galicia accreditation 2019-2022), grant GI-2033-TEOFPACC and ED431F2022/15, by European Union ERDF, and by the "Maria de Maeztu" Units of Excellence program MDM-2016-0692 and the Spanish Research State Agency, grant PID2019-105544GB-I00 and program "Ramon y Cajal", Grant No. RYC2019027017-I. FR was funded by the European Union's Horizon 2020 research and innovation programme under the Marie Skłodowska-Curie grant agreement No. 101065027.

References

[1] L. Evans and P. Bryant, Journal of Instrumentation **3** (08), S08001.
[2] T. Pierog *et al.*, Phys. Rev. C **92**, 034906 (2015).
[3] S. Ostapchenko, Phys. Rev. D **83**, 014018 (2011).
[4] F. Riehn *et al.*, Phys. Rev. D **102**, 063002 (2020).
[5] J. Albrecht *et al.*, Astrophysics and Space Science **367**, 27 (2022).
[6] The Pierre Auger Collaboration, Nuclear Instruments and Methods in Physics Research Section A: Accelerators, Spectrometers, Detectors and Associated Equipment **798**, 172 (2015).
[7] The Pierre Auger Collaboration (Pierre Auger Collaboration), Phys. Rev. Lett. **126**, 152002 (2021).
[8] The LHCf Collaboration, Journal of Instrumentation **3** (08), S08006.
[9] P. Younk and M. Risse, Astroparticle Physics **35**, 807 (2012).
[10] I. A. Goos, X. Bertou, and T. Pierog, Determination of high-energy hadronic interaction properties from observables of proton initiated extensive air showers (2023), arXiv:2304.08007 [hep-ex] .
[11] J. Matthews, Astroparticle Physics **22**, 387 (2005).
[12] L. Cazon, R. Conceição, and F. Riehn, Physics Letters B **784**, 68 (2018).
[13] L. Cazon, R. Concei ç ao, M. A. Martins, and F. Riehn, Phys. Rev. D **103**, 022001 (2021).
[14] T. Bergmann *et al.*, Astroparticle Physics **26**, 420 (2007).